Ortho and Para Hydrogen Dimers on G/SiC(0001): combined STM and DFT study

P. Merino[1], M. Švec[2], J. I. Martínez[3], P. Mutombo[2],C. Gonzalez[4] , J. A. Martín-Gago[1,3], P.L. de Andres,[3] P. Jelinek [2,5]*

[1] Centro de Astrobiología INTA-CSIC, Carretera de Ajalvir, km. 4, ES-28850 Madrid, Spain.

[2] Institute of Physics, Academy of Sciences of the Czech Republic, Cukrovarnicka 10, CZ-16200 Prague, Czech Republic.

[3] Instituto de Ciencia de Materiales de Madrid CSIC, c/ Sor Juana Inés de la Cruz, ES-28049 Madrid, Spain.

[4] Departamento de Fisica, Universidad de Oviedo, ES-33006, Spain.

[5] Graduate School of Engineering, Osaka University, 2-1 Yamada-Oka, Suita, Osaka 565-0871, Japan

**Present Adress Max-Planck Institute für Festkörperforschung, Heisenbergstr. 1, 70569 Stuttgart, Germany.*

KEYWORDS: Graphene, SiC, Hydrogen adsorbates, STM, DFT

The hydrogen (H) dimer structures formed upon room-temperature H adsorption on single layer graphene (SLG) grown on SiC(0001) are addressed using a combined theoretical-experimental approach. Our study includes density functional theory (DFT) calculations for the full $(6\sqrt{3}x6\sqrt{3})R30^{o}$ unit cell of the SLG/SiC(0001) substrate and atomically resolved scanning tunneling microscopy images determining simultaneously the graphene lattice and the internal

structure of the H adsorbates. We show that H atoms normally group in chemisorbed coupled structures of different sizes and orientations. We make an atomic scale determination of the most stable experimental geometries, the *small dimers* and *ellipsoid*-shaped features, and we assign them to hydrogen adsorbed in *para*-dimers and *ortho*-dimers configuration, respectively, through comparison with the theory.

INTRODUCTION

In the recent years, graphene hydrogenation has attracted increased attention for several reasons. First, storage of hydrogen (H) on carbonaceous materials has been considered a reasonable and safe route to store enough H to fulfill the conditions required for clean generation of energy [1 2 3]. Second, H can open a bandgap in graphene, a necessary step towards implantation of graphene in the design of novel electronic devices. Third, from an astronomical point of view, the interaction of H with graphitic surfaces has been proposed as a plausible explanation of the abundance of molecular H and polycyclic hydrocarbons in space [4 5 6 7]. Finally, H makes a simple probe to analyze the chemistry of graphene functionalization, yielding the unique possibility to study structural and electronic effects of this fundamental process without further difficulties of more complex adsorbates [8]. Therefore a thorough understanding of the hydrogenation/dehydrogenation process and H-C interaction on graphitic surfaces down to the atomic level is of great relevance both from an applied and a fundamental perspective.

Early scanning tunneling microscope (STM) experiments discovered that atomic H can chemisorb on the surface of highly oriented pyrolitic graphite (HOPG) in the form of dimers and small clusters [9 10 11]. These H structures can be removed from the surface by annealing to 500-600 K and present energetic pathways that favor molecular H_2 recombination. Later, it was also noticed that H adsorbs on the basal plane of single layer graphene (SLG) on different substrates. H adsorbed on SLG epitaxially grown on SiC(0001) forms small structures apparently identical to the ones observed on HOPG [12 13]. But, in addition to the structures observed in HOPG, single H atoms –monomers- are also spotted on SLG/SiC(0001) while absent in HOPG. These findings contrast with the behavior of H adsorbates on graphene epitaxialy grown on some metallic

surfaces. Experiments of hydrogenated graphene grown on Ir(111) combined with ab-initio calculations showed that H forms higher-order agglomerates and big clusters – rather than dimers - following the graphene Moiré as a template [2 14 15] .

From a theoretical point of view, H chemisorbs on top of a C atom within the graphene lattice and breaks the sp^2 original hybridization towards a sp^3 orbital arrangement. Several exciting properties of the adsorption of H atoms on SLG have been theoretically studied [16 17 18 19 20 21], including the full hydrogenization, resulting in the so called graphane, the 2D hydrocarbon [22] and the colossal enhancement of spin-orbit coupling [23]. However, a precise theoretical description of SLG epitaxially grown on substrates is still a challenge, due to the large number of atoms of the substrate involved in the usually large experimental graphene unit cells. Most of theprevious DFT studies of H adsorbed on graphene assume the role of the underlying substrate to be small and do not include it in the calculations [24 18 21]. However this assumption has not necessarily need to be true; attempts to theoretically describe the adsorption of H on graphene grown on transition metals [25] found that the interaction between graphene and metal alters the properties of SLG and therefore the H adsorption. On the other hand, the electronic properties of epitaxial graphene grown on SiC(0001) are close to the ones of free-standing graphene samples [26 27], and hence one can attain similar reactivities with adsorbates, but the large size of the pseudoperiodic $(6\sqrt{3}x6\sqrt{3})R30^{o}$ unit cell appearing underneath graphene complicates its study with ab-initio calculations. To the best of our knowledge there are no DFT calculations of H adsorbed on the full $(6\sqrt{3}x6\sqrt{3})R30^{0}$ unit cell and the only theoretical study of H adsorption on SiC(0001) was performed using an artificially smaller (3x3) unit cell [28].

In this work, we employ a combined experimental and theoretical approach to investigate the H dimer adsorption on the SLG/SiC(0001) surface in great detail. Atomically resolved STM

images are confronted with advanced DFT calculation including for the first time the $(6\sqrt{3}x6\sqrt{3})R30^{o}$ unit cell of the SiC(0001) substrate. The high resolution STM images allow us to determine the exact adsorption positions of H atoms on the graphene lattice. The most frequent experimental H dimer structures are positively identified using STM simulations as *ortho* and *para* H dimers.

METHODS

Experiments were carried out in a variable temperature scanning tunneling microscope (VT-STM) system with a base pressure of $5x10^{-11}$ mbar. We used research grade n-type Si terminated 6H-SiC(0001) samples cut from a wafer with a diamond tip. After degassing, the samples were cleaned by repeated cycles of annealing at 800˚C under a Si flux obtained from a Si source with a deposition rate of ≈0.1ML/min. This process typically leads to a (3x3) reconstruction observed by a sharp low energy electron diffraction (LEED) pattern. Further annealing at temperatures over 950˚C resulted in a partial depletion of Si atoms from the surface and the formation of a sharp $(\sqrt{3}x\sqrt{3})R30^{\circ}$ LEED pattern. Graphene was grown by further annealing at temperatures above 1100˚C. Typically SLG coexist with the $(6\sqrt{3}x6\sqrt{3})R30^{\circ}$ surface structure of 6H-SiC(0001), so called buffer layer. Repeated annealing of the samples at temperatures up to 1200˚C for 5-10 minutes resulted in an extensive growth of SLG and the apparition of some regions of bilayer graphene (BLG) [29]. An atomic H source (TECTRA GmBH) was used for H dissociation inside the UHV chamber. In our experimental setup, the flux is $5x10^{14}$ atoms/cm^2 on a sample located at 10 cm from the end of the capillary. The samples were exposed to the H flux for 10 minutes while being held at room temperature (RT). After dosing H, the samples were transferred to the STM where images have been obtained in the constant current mode using

standard etched tungsten tips. Typical bias voltages have ranged from +0.2V to -0.2V (positive meaning tunneling from the tip into the sample), with tunneling intensities up to 1nA.

We performed Density Functional Theory (DFT) calculation using the tight-binding FIREBALL code which is based on an optimized spatially-confined pseudo-atomic basis set. The code uses simulated thermal vibrations enabling the system to explore a bigger range of energetic configurations in order to avoid the local minima. All the calculations were based on the local density approximation formalism. To describe the Si and C atoms, sp basis sets were used. For the hydrogen atoms we chose an extended double basis set. The pseudo-atomic basis functions had the following cutoff radii:R(Si,s)=6.0 a.u, R(Si,p)=6.0 a.u., R(C,s)=4.5 a.u., R(C,p)=4.5 a.u and R(H,s,s)=4.5 a.u. The Brillouin zone was sampled only in the Γ point. The supercell was constructed of four $(6\sqrt{3}x6\sqrt{3})R30^{\circ}$ SiC bilayers terminated by hydrogen to maintain the charge balance. The cell was capped by a honeycomb carbon mesh, which strongly buckles upon relaxation, the buffer layer. On top of it, we placed a SLG with chemisorbed H dimers on top of atomic carbon positions. All the atoms were allowed to relax except for the last SiC bilayer and hydrogen layers. The C-H bond length of the capping H atoms was set to 1.2 Å. The stacking of the SiC bilayers corresponded to the 4H-SiC. The lattice parameter of the SiC unit cell was taken from previous works [30].

The STM simulations of the atomic hydrogen dimers configurations were carried out within the Green's function formalism. The Green's functions used to determine the tunneling current were obtained with the Fireball code. A pyramid-like tip derived from W(100) surface was employed to carry out the simulations. The local density of states of the W atoms of the tip were calculated with the Fireball code using a spd basis set. The following cutoff radii were used:R(W,s)=4.7 a.u, R(W,p)=5.2 a.u, R(W,d)=4.7 a.u. Furthermore, we used the previous cutoff radii to obtain the

projected density of states of the surface atoms. Note that the projected densities are used in the calculation of the tunneling current. All the STM maps were simulated in constant-height mode at bias voltage of ± 0.3V and tip-sample distance of 3.5 Å unless stated otherwise. To corroborate the H configurations we have also calculated height profiles. These theoretical profiles were compared to experimental findings.

RESULTS AND DISCUSSION

Figure 1 shows large area STM image of atomic H adsorbates on graphene. To emphasize the H visualization we have used a double color scale where the topographically protruding objects are presented in blue scale while the lower regions are colored in grey (see the color scale in Fig. 1). Under this representation the H adsorbates emerge as blue agglomerates distributed on the graphene surface which appears in between the protrusions in grey scale. The H atoms are not observed to diffuse at RT but can be easily desorbed while scanning, in good agreement with previous results [9]. To avoid spontaneous tip-induced desorption, voltages between +3V and -3V must be used in the tunneling conditions during measurements. Applying voltage pulses above/below these values produce controlled voltage-induced desorption that can be used for nm-precise nano-patterning, as it was noticed by P. Sessi *et al.* [31]. In Fig. 1 there are 350 clusters in a total area of 1040 nm^2. Hence, we estimate a H coverage around 1.8%. The mean height of the adsorbates is 1.7Å, as extracted from a histogram analysis (data not shown). At the first glance, no well-ordered superstructure (i.e. crystallographic) is observed; the clusters appear randomly distributed or forming amorphous agglomerates. The hydrogen coverage can be tuned by changing the hydrogen exposition time during sample growth and can be locally diminished

by voltage manipulation, yielding to lower density of adsorbates. In the vicinities of the adsorbates graphene shows charge density oscillations with the (√3x√3)R30˚ periodicity due to quasiparticle scattering and interference with the H atoms [32]. We show an example of this behavior in the inset of Fig. 1.

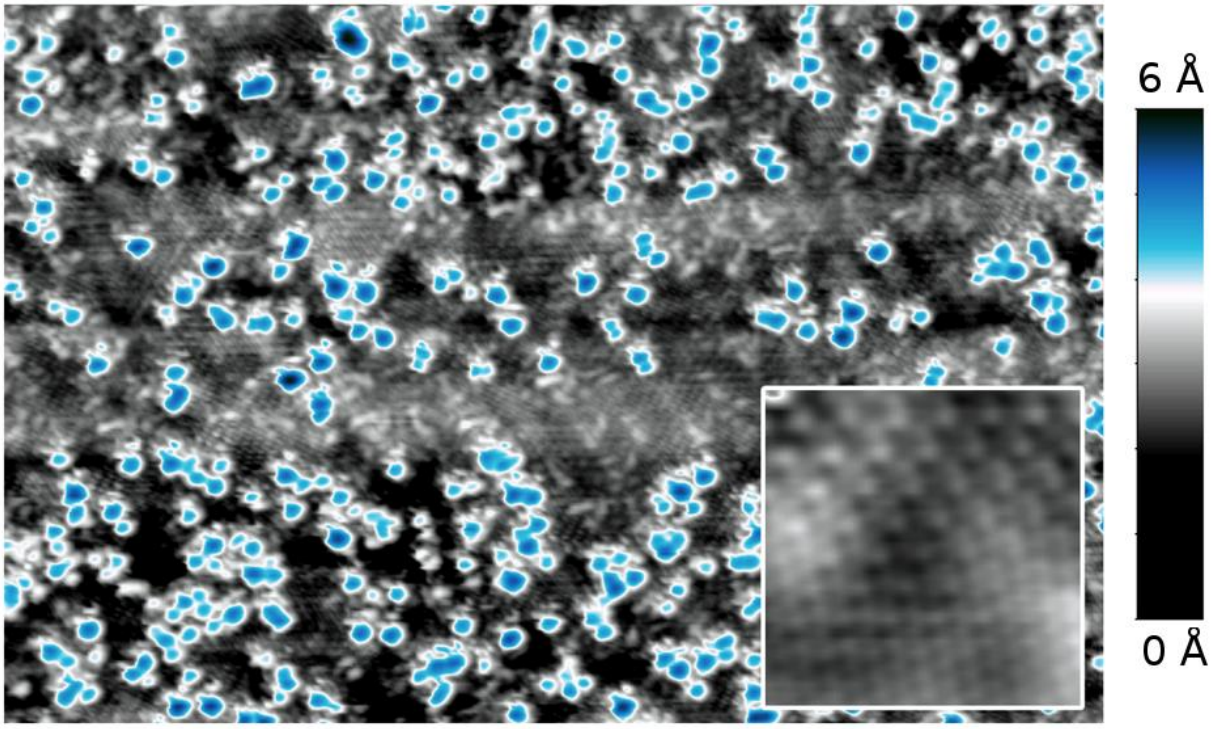

Figure 1. *STM image of more than 350 H adsorbate clusters on SLG/SiC(0001). V=-0.1V, I=1nA, 40x26nm^2 . The inset shows the (√3x√3)R30˚ periodicity due to quasiparticle scattering and interference with the H atoms, 3.5x3.5nm^2.*

We have taken high-resolution STM images of regions with small density of adsorbates to determine the precise atomic configuration of the most common hydrogen adsorption geometries. In Fig.2 a we observe the H adsorbates on atomically resolved graphene lattice. The

honeycomb structure is resolved together with the dangling bonds of the reconstruction underneath; this morphology corresponds to SLG on SiC [33] and will be discussed in detail later. The resolution in Fig. 2 a is exceptional due to a very sharp tip. This outstanding resolution offers us the possibility to determine the relative position of the H induced STM features with respect to the graphene atomic network. We will use this resolution to fully understand the adsorption geometries of the H clusters on graphene. Up to our knowledge, these are the first STM images that simultaneously resolve the SLG/SiC(0001) with atomic resolution together with the internal structure of the H adsorbates. In Fig. 2 b we have superimposed the atomic C honeycomb grid on top of the experimental STM image. One of the $[1\bar{1}20]$ surface crystallographic directions of graphene runs parallel to the vertical of the image. Positioning the graphene lattice with atomic precision is a very difficult task as drift effects lead to a situation where the distances are distorted in the different directions of the surface and in the different parts of the image. To overcome this problem we have determined the distortions in all the three independent $[1\bar{1}20]$ lattice directions and generated an accordingly deformed honeycomb lattice which is displayed in Fig. 2 b. We shall remark that the grid allows to locate the positions of more than 14000 C atoms.

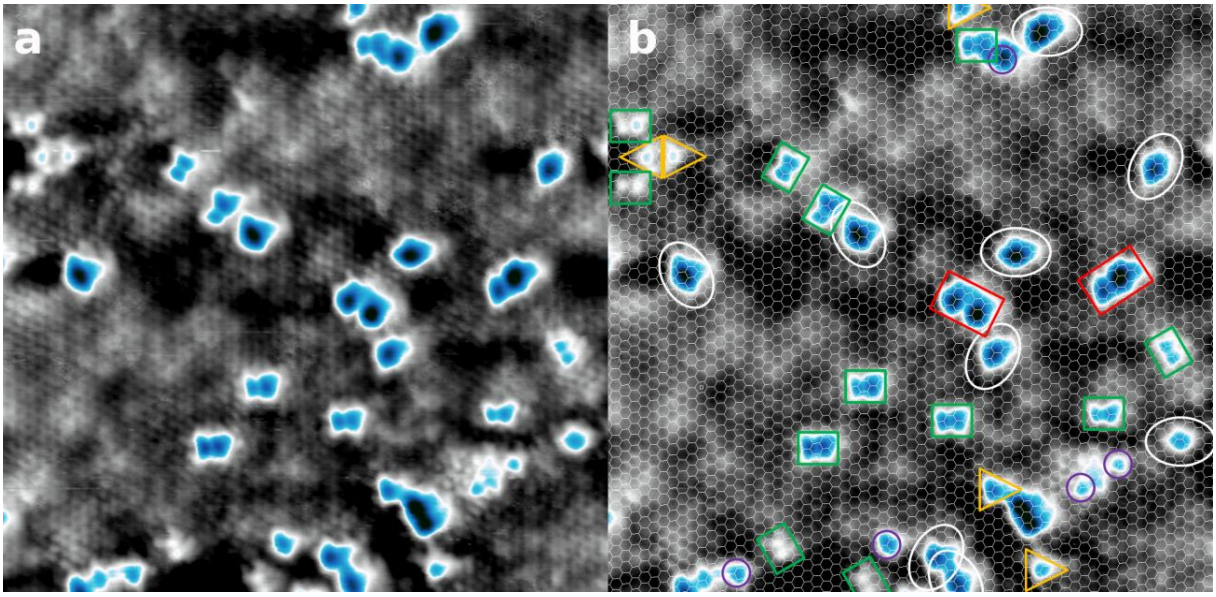

Figure 2: *High resolution STM images of H adsorbates on SLG forming small clusters. a. V=-0.3V, I=1nA, 12x12nm^2.b. Image where the atomic graphene grid has been superimposed and the clusters have been classified with a geometrical and a color code (see text).*

After placing the grid, we observe that only a limited number of atomic scale structures define the basic clusters which comprise the bigger agglomerates. We find that all adsorbates can be classified in terms of 5 basic building blocks, to facilitate their recognition we have used a geometrical color code to identify them: *small dimers* (enclosed by green rectangles), *big dimers* (red rectangles), *ellipsoids* (white ellipses), *trimers* (yellow triangles) and *monomers* (purple circles). Moreover, we find the rotationally equivalent orientations of the structures. In particular the three orientations of the *small dimers* (0°, 60°, and 120°) are shown in the Fig. 2 and two equivalent crystallographic structures are observed for the *big dimers* and *trimers*. *Ellipsoid* structures are also present in the three equivalent directions according to their substrate commensuration, but the absence of clear internal structure and the appearance of a plume-like feature along the scanning direction (the horizontal one) due to tip imperfections complicate

identification of its rotational position. Only after placing the graphene lattice over a high-resolution STM image their orientation is revealed. Remarkably, the majority of the structures found in our experiments are *small-dimers* (35%) and *ellipsoids* (20%), while *trimers*, *big-dimers*, *monomers* and bigger structures have a smaller probability of occurrence accounting for the 45% of the clusters.

In Fig. 3 a we present a high resolution STM image of a *small dimer* and *ellipsoid*, on an atomically resolved graphene surface. The *small dimer* possesses two slightly asymmetrical lobes with a mean apparent height of 1.4Å. The distance between the maxima of both lobes is 3.2Å. The *ellipsoid* structure presents a single maximum with average height of 1.7Å. The graphene atomic grid in Fig. 3 b provides an experimental hint of where the H atoms are atomically positioned. The first impression suggests that the two maxima of the *small dimer* are placed on top of diagonally opposed C atoms of one honeycomb ring. If we assume that each of the maxima is an H atom this configuration would correspond to *para*-configuration of the H couple on graphene [10 18]. The *ellipsoid* structure only presents one height maximum, but its large size implies that more than one H atom is involved. The simplest structure fulfilling symmetry and area considerations for the *ellipsoids* structure is the adsorption of two H atoms on first neighbor C atoms in the graphene lattice; this is known as *ortho*-configuration [10 18]. In Fig. 3 c we have schematically represented the *ortho* and *para* configurations of adsorbed H dimers in a ball-and-stick model. These structures are similar to the ones reported in the literature, where the experimental H-dimers on SLG/SiC(0001) are described simply as *ellipsoids* and where internal resolution within the clusters is rarely observed [12]. In their seminal work, Hornekær *et al.* identified the hydrogen *ortho-dimer* and *para-dimer* by STM experiments on H/HOPG [9 12]. In their analysis the experimental STM appearance of the *ortho-dimer* is described as an elongated

spheroid with a thin dark central structure (node) along the minor axis and the *para-dimer* is described as more rectangular and without any internal structure. According to our experimental observations the *ortho-dimer* is an ellipsoid structure with no internal structure and the *para-dimer* is a butterfly-shaped structure with an internal node. It is important to notice that tip smoothing effects can easily smear out the central node of the dimers and complicate the identification. To the best of our knowledge there are no more published STM work identifying single H-dimers to confront. We believe this illustrates how difficult it is to obtain atomically resolved STM images of H adsorbates on graphitic surfaces. Hornekær *et al.* describe the structures obtained in SLG/SiC(0001) identical to the ones reported in HOPG [12] [9] but the resolution presented in their SLG/SiC(0001) experiment is slightly worsened with respect to the one obtained at HOPG. To test the influence of the substrate and confirm whether or not it changes the aspect of the dimers in the STM images, DFT calculations of the *ortho* and *para* configurations on the full SLG/SiC(0001) become crucial.

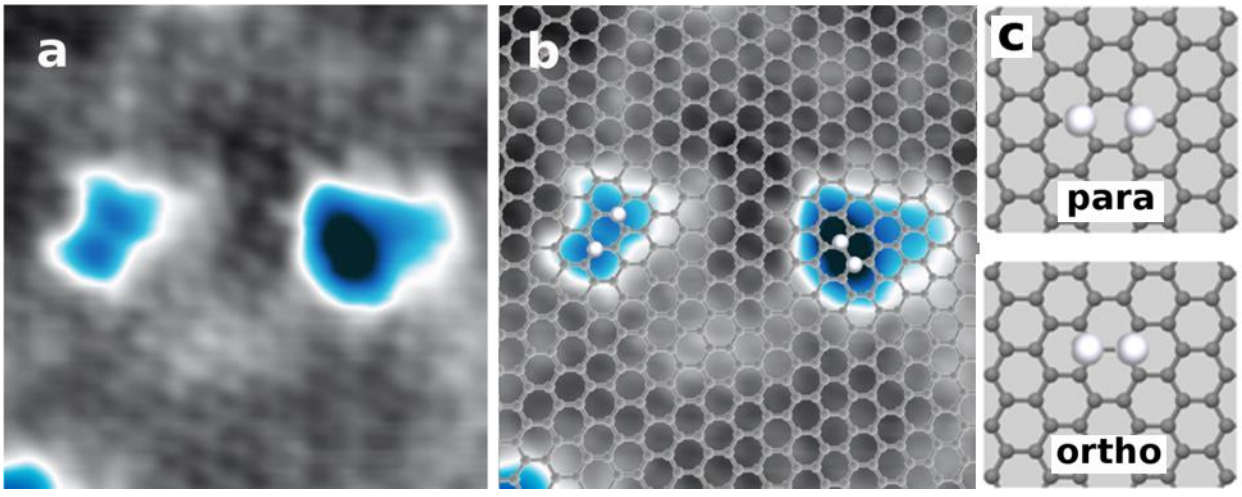

Figure 3: *High resolution STM images of H small dimers on SLG.* ***a****. V=-0.3V, I=1nA, 3.8x3.8nm*^{2}*.* ***b****. Image where the atomic graphene grid has been superimposed. A suggested*

position for the chemisorbed H is indicated. ***c****. Schematic representation of the model H dimers: para dimer (third-nearest neighbors) and ortho dimer (first-nearest neighbors)*

We have performed intensive DFT calculations of the different possible theoretical absorption geometries of H dimers including the $(6\sqrt{3}x6\sqrt{3})R30^{o}$ crystallographic structure of the substrate. The relaxation of this unit cell is computationally very demanding and several atomistic structures have been proposed [34] [35] [36]. In Fig. 4g we introduce a perspective view of our optimized SLG/$(6\sqrt{3}x6\sqrt{3})R30^{o}$ SiC unit cell. To fully reproduce the main experimental observations 1650 atoms are needed to be included in the calculations. The relaxed structure of the unit cell can be described as follows: four slabs of SiC pairs presenting an atomic configuration relatively close to the hexagonal SiC bulk configuration, Si-C bond distance of 1.9Å and SiC-SiC interlayer distance of 2.6Å, compared with experimental 1.89Å and 2.52 Å [37] [38]. The SiC slabs are capped by the buffer layer, a highly buckled honeycomb carbon mesh with a peak-to-peak corrugation of 1.1Å. This strong corrugation within the honeycomb carbon lattice of the buffer layer breaks the sp^2 hybridization and induces the bonding between some of the carbon atoms within this buffer layer and some of the Si atoms of the last "unperturbed" SiC slab underneath. Therefore the properties of the buffer layer are far from those of pristine graphene, although they both share the honeycomb carbon lattice as its basic structure [39] [40]. Finally, on top of all, at a vertical distance of 3.6Å over the buffer layer, we find a pure (13x13) sheet of SLG with a small corrugation of 0.19 Å. The H atoms are placed on top of graphene in either *para* or *ortho* configurations and the structure is optimized again. The basic geometrical parameters of the relaxed structures are summarized in Table 1

Vertical atomic position (Å)	Maximum value (Å)		Minimum value (Å)		Average (Å)	
	Para	Ortho	Para	Ortho	Para	Ortho
SLG	7.003	7.188	6.526	6.507	6.578	6.565
Buffer Layer	3.467	3.488	2.304	2.303	2.970	2.973
TOP-Si in last SiC bilayer	0.354	0.355	0.010	0.012	0.233	0.234
TOP-C in last SiC bilayer	-0.240	-0.236	-0.486	-0.486	-0.374	-0.372

Table 1: *Maximum, minimum and average vertical atomic positions of C in SLG/(6√3x6√3)R30° SiC, as extracted from the theoretical calculations of the para and ortho configurations of hydrogen dimers.*

To test the validity of our model for the SLG/(6√3x6√3)R30° SiC structure we have also performed STM simulations of the clean surface. In Fig.4 we present a qualitative comparison of the theoretically simulated constant-height images and the experimental topography. For the calculation, we used the fully relaxed (6√3x6√3)R30° unit cell with the 13x13 SLG on top. In Fig.4 a,b is shown the characteristic contrast fingerprint of graphene and a long-range Moire-like modulation originating from the strong corrugation of the buffer layer, for the empty and filled states, respectively. The typical localized features (i.e. subsurface dangling bonds) present in the representative experimental images (Fig.4 e,f) are, nonetheless, not reproduced in the basic calculation. The DFT shows that some of the Si atoms under the buffer layer are not fully saturated by the C atoms in the buffer layer. Therefore, dangling bonds are present at the

interface, but at the normal buffer layer - SLG distance (3.6 Å), their spatial extent does not reach far enough to influence the STM image. However, by moving the SLG artificially towards the buffer layer and running the simulation again, we could also reproduce the characteristic features and associate them with the unsaturated Si bonds. The features appear when the SLG is moved by 0.4 Å and increase their intensity when moving further. The Fig.4 c,d show the simulation with the SLG moved by 0.6 Å for the empty and filled states, respectively.

The need for the artificial change of SLG - buffer layer distance to reproduce the experimental data can be justified as an offset in the distance produced by neglecting the van der Waals contribution in the calculations. Another contribution could be a relaxation of the interlayer distance caused by the proximity of the scanning probe. More investigation would be needed to explain this phenomenon unambiguously. Nevertheless, we can conclude that the general agreement between the experiments and theory for the SLG/($6\sqrt{3}$x$6\sqrt{3}$)R30° system is in overall very good. Given the good agreement between calculations and experiments we believe our approach is appropriate to further study the adsorption of H dimers on SLG/($6\sqrt{3}$x$6\sqrt{3}$)R30°.

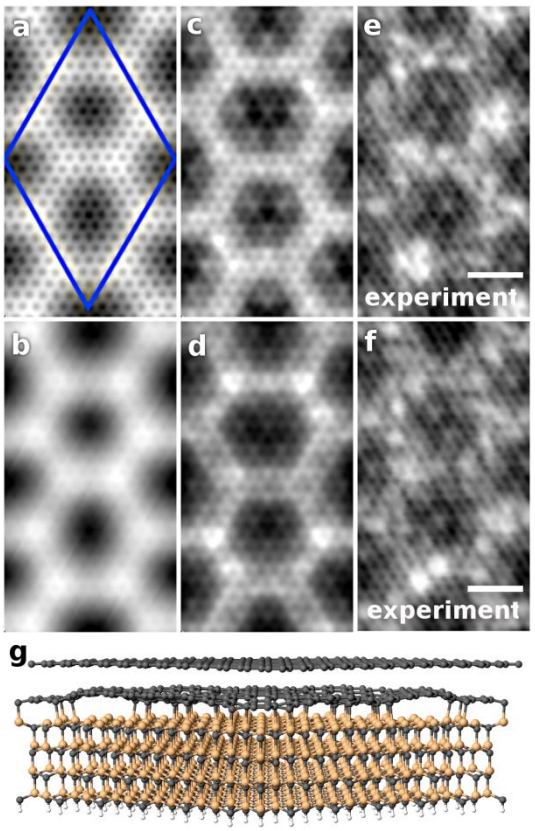

Figure 4: (a-d) *the simulated STM contrast qualitatively compared to experimental images in (e),(f). (g) the model used for the simulation was the fully relaxed model of 4H-SiC(0001) SLG/(6√3x6√3)R30°unit cell with 13x13 single layer graphene on top. Basic theoretical images were obtained in constant height mode with the following parameters:* ***(a)*** *+30 mV,* ***(b)*** *-50 mV. Better qualitative agreement with the experiment was achieved after artificially moving the graphene layer by 0.6 Å towards the buffer layer for* ***(c)*** *30 mV and* ***(d)*** *-50 mV. The characteristic experimental topography examples of the unit cell in* ***(e)***,***(f)*** *were taken from two different locations at -1.1V, the scale bars corresponds to 1nm.*

In Fig. 5a we present the ball-and-stick representation of the relaxed structure of a hydrogen *para-dimer* on top of the full (6√3x6√3)R30° unit cell used in our calculations. The inset magnifies the region of adsorption of the two H atoms. One can notice that the C atoms just

below the H atoms (represented as grey and white spheres respectively) are lifted strongly from their original unrelaxed positions. Our theoretical results indicate that the C atoms in the vicinity of the H atoms are strongly affected by the formation of the C-H bonds. The heigth difference between the highest and lowest atoms in the SLG equals 0.51Å and 0.68 Å for the *para* and *ortho* configurations respectively. Furthermore, the buffer layer and the topmost SiC bilayers are locally buckled in the same way for the two types of H structures. The vertical distortion among C atoms belonging to the buffer layer was found to be 1.16 Å for the *para* and 1.18 Å for the *ortho* configurations. Within the topmost SiC bilayer, the Si atom heighth varys more (0.34Å) than the heighths of C atoms (0.24Å). Using the average atomic position as reference, one finds that the interlayer distances of SLG-buffer layer and buffer layer-top Si layer are 3.60 and 2.73Å respectively. Moreover the vertical separation between Si and C within SiC top layer is approximately 0.60 Å. Interestingly, the H-atoms in the *ortho* and *para* configuration are elevated 1.77 and 1.66 Å above the position of the average layer. Based on the computed total energy of both structures, we can assert that the *ortho* configuration is more favorable than the *para*-configuration by 0.016 eV.

In Fig. 5 b we present STM images of the experimental *ortho* and *para* dimer configurations in comparison to simulated STM images. The agreement between the images for the experimental short dimer and the theoretical *para-dimer* is very good; the minima appearing in the experimental images between both lobes that gives its characteristic butterfly-shaped aspect to short dimers, is well resolved in the theoretically simulated images. The apparition of a node in the *para-dimer* differs from previous STM simulation studies of H dimers on HOPG [10]. The experimental *ellipsoid* structure is very similar to the theoretically simulated STM image of the *ortho-dimer*.

To go beyond visual comparison, we have performed profile analysis of the size and height of experimental and theoretical H-dimer structures. The real H dimers are adsorbed at different locations within the $(6\sqrt{3}x6\sqrt{3})R30^{o}$ unit cell of the substrate, resulting in slight structural differences. Typically, there are small differences in apparent heights and in lateral sizes, which are in the order of 0.1Å and 0.3Å, respectively. For this purpose we averaged the profiles of *small dimers* and *ellipsoids*. In the right part of Fig 5b we present this averaged profile (solid black line) together with the theoretically calculated one (dashed red line); we have also represented the maximum deviation as a grey colored area around the experimental profile. The agreement between experiments and theory is very good and the distance between maxima for the *short dimer* as well as the total height and size for both dimers is well reproduced (*ortho-dimer*: experimental height 1.6±0.3Å vs. theoretical height 1.75Å; *para-dimer*: experimental height 1.4±0.3Å vs. theoretical height 1.4Å). The combination of these results with the high resolution STM images including the honeycomb lattice of the SLG substrate (see Fig. 3) proves that the short dimer corresponds to coupled H atoms adsorbed in a *para*-configuration, while the experimental ellipsoid structures correspond to coupled H atoms in the *ortho*-configuration.

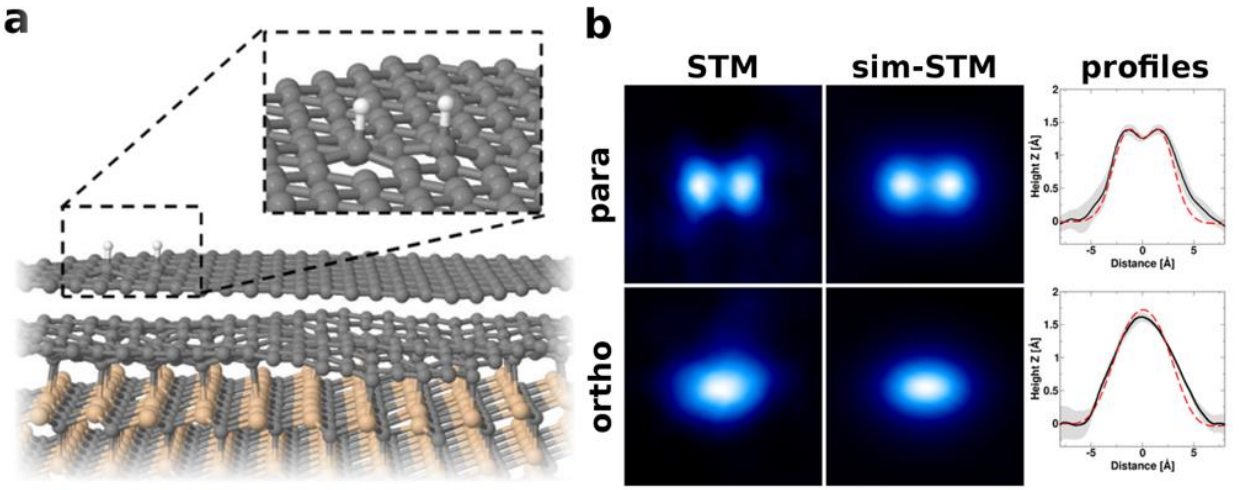

Figure 5: a. *Ball and stick model of a hydrogen dimer adsorbed on top of SLG/(6√3x6√3)R30°. The inset highlights the H adsorption region.* **b.** *Experimental and simulated STM images of the para and ortho hydrogen dimer configurations. The graphs show a profile analysis of the different theoretical structures (red dashed line) together with the experimental curves (black solid line) and the deviation (grey area).*

The calculated energy difference between *ortho-dimers* and *para-dimers* is only 0.016 eV. This energy is smaller than the thermal excitation at room temperature (0.025 eV) and therefore conversion between both types of dimers could be expected. However this is not observed during the experiments, most likely due to the high energy barriers that have to be overcome between chemisorbed states. Interestingly we have found energy differences when the dimers are adsorbed in different positions within the complex unit cell. In particular, for the *para-dimers*, the energy of the structures adsorbed in the *higher* regions of the (6√3x6√3)R30° – the region of the SLG/SiC(0001) unit cell appearing brighter in the STM images- is -0.230 eV more favored than adsorption within the *lower* regions of the unit cell, in good agreement with the experimental observations [12]. This demonstrates that for the particular configurations, absorption

site in the $(6\sqrt{3}x6\sqrt{3})R30^{o}$ may play a bigger role than the dimer type. We shall remark that van der Waals forces (typically in the ~1 meV range) play a negligible role in hydrogen adsorption since chemisorption (typically in the ~1 eV range) is the driving mechanism. This is in contrast to physisorbed adsorbates on the same surface where van der Waals interactions might play a significant role[41]. A systematic DFT and STM study would be required for a better understanding of the energetic interplay between adsorption position and structural conformation. Nevertheless, these observations put forward the importance of a full substrate description in the calculation. We have also performed calculations without the buffer layer in order to test the importance of its role. In this case the calculations indicate an energetic preference of 0.009 eV –to compare with the 0.016 eV including the unit cell- towards the *ortho* configuration. The energies of the dimers on freestanding SLG keep the energetic preference of the *ortho* configuration, but the energy difference between *ortho* and *para* configurations diminish compared with the calculation including with the full SLG/$(6\sqrt{3}x6\sqrt{3})R30^{0}$ unit cell of the substrate.

CONCLUSIONS

We analyzed atomically resolved STM images of the small clusters appearing on SLG/$(6\sqrt{3}x6\sqrt{3})R30^{0}$ upon atomic hydrogen exposition. Combined experimental results and advanced theoretical calculations allowed a full determination of the adsorption geometries of the most common structures: *short dimers* and *ellipsoids*. Our study overcomes the difficulties appearing in the correct identification of hydrogen clusters chemisorbed on SLG grown on SiC(0001) and identifies the short dimers appearing on SLG/SiC(0001) as *para-dimers*, while

the *ellipsoid* structures as *ortho-dimers*. Comparison of the experiments with the calculations revealed that the STM images show an important electronic contribution of the substrate. The calculated total energies reproduce qualitatively the observed preferred sticking position within the unit cell. The energy difference between *ortho* and *para* configurations is smaller than the thermal excitation at RT. The adsorption position within the SLG/SiC(0001) unit cell is found to be more important than the dimer type in the energy calculations. In particular, for the *para-dimer*, the difference between adsorption energy in the higher regions and the lower regions of the Moiré-like modulation can be as big as 0.230 eV Our combined experimental-theoretical approach can be extended to *monomers, trimers, big dimers* and other clusters for a precise understanding of the H/SLG/($6\sqrt{3}$x$6\sqrt{3}$)R30^0 system.

AUTHOR INFORMATION

Corresponding Author

*E-mail: p.merino@fkf.mpg.de

Notes

The author declare no competing financial interest

AKNOWLEDGEMENTS

P.M acknowledges financial support from a R. C. Rodes grant. The research leading to these results has received funding from the European Union Seventh Framework Program under grant agreement n°604391 Graphene Flagship. We acknowledge financial support by the Spanish project MAT2011-26534. M. S, P.M and P.J acknowledge the financial support of GACR project no. 14-02079S.

REFERENCES

1. Elias, D. C.; Nair, R. R.; Mohiuddin, T. M. G.; Morozov, S. V.; Blake, P.; Halsall, M. P.; Ferrari, A. C.; Boukhvalov, D. W.; Katsnelson, M. I.; Geim, A. K.; Novoselov, K. S., Control of Graphene's Properties by Reversible Hydrogenation: Evidence for Graphane. *Science* **2009,** *323*, 610-613.
2. Balog, R.; Jorgensen, B.; Nilsson, L.; Andersen, M.; Rienks, E.; Bianchi, M.; Fanetti, M.; Laegsgaard, E.; Baraldi, A.; Lizzit, S.; Sljivancanin, Z.; Besenbacher, F.; Hammer, B.; Pedersen, T. G.; Hofmann, P.; Hornekaer, L., Bandgap opening in graphene induced by patterned hydrogen adsorption. *Nat. Mater.* **2010,** *9*, 315-9.
3. Subrahmanyam, K. S.; Kumar, P.; Maitra, U.; Govindaraj, A.; Hembram, K. P. S. S.; Waghmare, U. V.; Rao, C. N. R., Chemical storage of hydrogen in few-layer graphene. *Proc. Natl. Acad. Sci. U.S.A* **2011,** *108*, 2674-2677.
4. Merino, P.; Švec, M.; Martinez, J. I.; Jelinek, P.; Lacovig, P.; Dalmiglio, M.; Lizzit, S.; Soukiassian, P.; Cernicharo, J.; Martin-Gago, J. A., Graphene etching on SiC grains as a path to interstellar polycyclic aromatic hydrocarbons formation. *Nat. Commun.* **2014,** *5,* 1-9.
5. Cuppen, H. M.; Hornekær, L., Kinetic Monte Carlo studies of hydrogen abstraction from graphite. *J. Chem. Phys.* **2008,** *128*, 1-12.
6. Vidali, G., H2 Formation on Interstellar Grains. *Chem. Rev.* **2013,** *113*, 8762-8782.
7. Cuppen, H. M.; Karssemeijer, L. J.; Lamberts, T., The Kinetic Monte Carlo Method as a Way To Solve the Master Equation for Interstellar Grain Chemistry. *Chem. Rev.* **2013,** *113*, 8840-8871.
8. de Andres, P. L.; Vergés, J. A., First-principles calculation of the effect of stress on the chemical activity of graphene. *Appl. Phys. Lett.* **2008,** *93*, 1-3.
9. Hornekær, L.; Šljivančanin, Ž.; Xu, W.; Otero, R.; Rauls, E.; Stensgaard, I.; Lægsgaard, E.; Hammer, B.; Besenbacher, F., Metastable Structures and Recombination Pathways for Atomic Hydrogen on the Graphite (0001) Surface. *Phys. Rev. Lett.* **2006,** *96*, 156104.
10. Hornekær, L.; Rauls, E.; Xu, W.; Šljivančanin, Ž.; Otero, R.; Stensgaard, I.; Lægsgaard, E.; Hammer, B.; Besenbacher, F., Clustering of Chemisorbed H(D) Atoms on the Graphite (0001) Surface due to Preferential Sticking. *Phys. Rev. Lett.* **2006,** *97*, 186102.
11. Hornekær, L.; Xu, W.; Otero, R.; Lægsgaard, E.; Besenbacher, F., Long range orientation of meta-stable atomic hydrogen adsorbate clusters on the graphite(0001) surface. *Chem. Phys. Lett.* **2007,** *446*, 237-242.
12. Balog, R.; Jørgensen, B.; Wells, J.; Lægsgaard, E.; Hofmann, P.; Besenbacher, F.; Hornekær, L., Atomic Hydrogen Adsorbate Structures on Graphene. *J. Am. Chem. Soc.* **2009,** *131*, 8744-8745.
13. Guisinger, N. P.; Rutter, G. M.; Crain, J. N.; First, P. N.; Stroscio, J. A., Exposure of Epitaxial Graphene on SiC(0001) to Atomic Hydrogen. *Nano Lett.* **2009,** *9*, 1462-1466.
14. Ulstrup, S.; Nilsson, L.; Miwa, J. A.; Balog, R.; Bianchi, M.; Hornekær, L.; Hofmann, P., Electronic structure of graphene on a reconstructed Pt(100) surface: Hydrogen adsorption, doping, and band gaps. *Phys. Rev. B* **2013,** *88*, 125425.
15. Balog, R.; Andersen, M.; Jørgensen, B.; Sljivancanin, Z.; Hammer, B.; Baraldi, A.; Larciprete, R.; Hofmann, P.; Hornekær, L.; Lizzit, S., Controlling Hydrogenation of Graphene on Ir(111). *ACS Nano* **2013,** *7*, 3823-3832.
16. SljivanCanin, Z.; Rauls, E.; Hornekaer, L.; Xu, W.; Besenbacher, F.; Hammer, B., Extended atomic hydrogen dimer configurations on the graphite(0001) surface. *J. Chem. Phys.* **2009,** *131*, 084706.

17. Casolo, S.; Lovvik, O. M.; Martinazzo, R.; Tantardini, G. F., Understanding adsorption of hydrogen atoms on graphene. *J. Chem. Phys.* **2009,** *130*, 054704.
18. Ferro, Y.; Teillet-Billy, D.; Rougeau, N.; Sidis, V.; Morisset, S.; Allouche, A., Stability and magnetism of hydrogen dimers on graphene. *Phys. Rev. B* **2008,** *78*, 085417.
19. McKay, H.; Wales, D. J.; Jenkins, S. J.; Verges, J. A.; de Andres, P. L., Hydrogen on graphene under stress: Molecular dissociation and gap opening. *Phys. Rev. B* **2010,** *81*, 075425.
20. Huang, L. F.; Cao, T. F.; Gong, P. L.; Zeng, Z.; Zhang, C., Tuning the adatom-surface and interadatom interactions in hydrogenated graphene by charge doping. *Phys. Rev. B* **2012,** *86*, 125433.
21. Šljivančanin, Ž.; Andersen, M.; Hornekær, L.; Hammer, B., Structure and stability of small H clusters on graphene. *Phys. Rev. B* **2011,** *83*, 205426.
22. Sofo, J. O.; Chaudhari, A. S.; Barber, G. D., Graphane: A two-dimensional hydrocarbon. *Phys. Rev. B* **2007,** *75*, 153401.
23. Gmitra, M.; Kochan, D.; Fabian, J., Spin-Orbit Coupling in Hydrogenated Graphene. *Phys. Rev. Lett.* **2013,** *110*, 246602.
24. Khazaei, M.; Bahramy, M. S.; Ranjbar, A.; Mizuseki, H.; Kawazoe, Y., Geometrical indications of adsorbed hydrogen atoms on graphite producing star and ellipsoidal like features in scanning tunneling microscopy images: Ab initio study. *Carbon* **2009,** *47*, 3306-3312.
25. Andersen, M.; Hornekær, L.; Hammer, B., Graphene on metal surfaces and its hydrogen adsorption: A meta-GGA functional study. *Phys. Rev. B* **2012,** *86*, 085405.
26. Berger, C.; Song, Z.; Li, T.; Li, X.; Ogbazghi, A. Y.; Feng, R.; Dai, Z.; Marchenkov, A. N.; Conrad, E. H.; First, P. N.; de Heer, W. A., Ultrathin Epitaxial Graphite: 2D Electron Gas Properties and a Route toward Graphene-based Nanoelectronics. *J. Phys. Chem. B* **2004,** *108*, 19912-19916.
27. Berger, C.; Song, Z.; Li, X.; Wu, X.; Brown, N.; Naud, C.; Mayou, D.; Li, T.; Hass, J.; Marchenkov, A. N.; Conrad, E. H.; First, P. N.; de Heer, W. A., Electronic Confinement and Coherence in Patterned Epitaxial Graphene. *Science* **2006,** *312*, 1191-1196.
28. Lee, B.; Han, S.; Kim, Y.-S., First-principles study of preferential sites of hydrogen incorporated in epitaxial graphene on 6H-SiC(0001). *Phys. Rev. B* **2010,** *81*, 075432.
29. Forbeaux, I.; Themlin, J. M.; Debever, J. M., Heteroepitaxial graphite on 6H-SiC(0001): Interface formation through conduction-band electronic structure. *Phys. Rev. B* **1998,** *58*, 16396-16406.
30. Telychko, M.; Mutombo, P.; Ondráček, M.; Hapala, P.; Bocquet, F. C.; Kolorenč, J.; Vondráček, M.; Jelínek, P.; Švec, M., Achieving High-Quality Single-Atom Nitrogen Doping of Graphene/SiC(0001) by Ion Implantation and Subsequent Thermal Stabilization. *ACS Nano* **2014,** *8*, 7318-7324.
31. Sessi, P.; Guest, J. R.; Bode, M.; Guisinger, N. P., Patterning graphene at the nanometer scale via hydrogen desorption. *Nano Lett.* **2009,** *9*, 4343-7.
32. Rutter, G. M.; Crain, J. N.; Guisinger, N. P.; Li, T.; First, P. N.; Stroscio, J. A., Scattering and Interference in Epitaxial Graphene. *Science* **2007,** *317*, 219-222.
33. Rutter, G. M.; Guisinger, N. P.; Crain, J. N.; Jarvis, E. A. A.; Stiles, M. D.; Li, T.; First, P. N.; Stroscio, J. A., Imaging the interface of epitaxial graphene with silicon carbide via scanning tunneling microscopy. *Phys. Rev. B* **2007,** *76*, 235416.
34. Chen, W.; Chen, S.; Zhang, H. L.; Xu, H.; Qi, D. C.; Gao, X. Y.; Loh, K. P.; Wee, A. T. S., Probing the interaction at the C60–SiC nanomesh interface. *Surf. Sci.* **2007,** *601*, 2994-3002.

35. Qi, Y.; Rhim, S. H.; Sun, G. F.; Weinert, M.; Li, L., Epitaxial Graphene on SiC(0001): More than Just Honeycombs. *Phys. Rev. Lett.* **2010,** *105*, 085502.
36. Nemec, L.; Blum, V.; Rinke, P.; Scheffler, M., Thermodynamic Equilibrium Conditions of Graphene Films on SiC. *Phys. Rev. Lett.* **2013,** *111*, 065502.
37. Hass, J.; Feng, R.; Millán-Otoya, J. E.; Li, X.; Sprinkle, M.; First, P. N.; de Heer, W. A.; Conrad, E. H.; Berger, C., Structural properties of the multilayer graphene system as determined by surface x-ray diffraction. *Phys. Rev. B* **2007,** *75*, 214109.
38. Krausslich, J.; Bauer, A.; Wunderlich, B.; Goetz, K. In *Lattice parameter measurements of 3C-SiC thin films grown on 6H-SiC (0001) substrate crystals*, Materials Science Forum, Transtec Publications; 1999: 2001; 319-322.
39. Riedl, C.; Coletti, C.; Iwasaki, T.; Zakharov, A. A.; Starke, U., Quasi-Free-Standing Epitaxial Graphene on SiC Obtained by Hydrogen Intercalation. *Phys. Rev. Lett.* **2009,** *103*, 246804.
40. Riedl, C.; Coletti, C.; Starke, U., Structural and electronic properties of epitaxial graphene on SiC(0 0 0 1): a review of growth, characterization, transfer doping and hydrogen intercalation. *J. Phys. D: Appl. Phys.* **2010,** *43*, 374009.
41. Švec, M.; Merino, P.; Dappe, Y. J.; González, C.; Abad, E.; Jelínek, P.; Martín-Gago, J. A., van der Waals interactions mediating the cohesion of fullerenes on graphene. *Phys. Rev. B* **2012,** *86*, 121407.

Table of contents